Palmitoylation Controls Dopamine Transporter Kinetics, Degradation, and Protein Kinase C-dependent Regulation*

James D. Foster and Roxanne A. Vaughan[1]

From the Department of Biochemistry and Molecular Biology, University of North Dakota School of Medicine and Health Sciences, Grand Forks, North Dakota 58202-9037

Palmitoylation is a lipid modification that confers diverse functions to target proteins and is a contributing factor for many neuronal diseases. In this study, we demonstrate using [^{3}H]palmitic acid labeling and acyl-biotinyl exchange that native and expressed dopamine transporters (DATs) are palmitoylated, and using the palmitoyl acyltransferase inhibitor 2-bromopalmitate (2BP), we identify several associated functions. Treatment of rat striatal synaptosomes with 2BP using lower doses or shorter times caused robust inhibition of transport V_{max} that occurred with no losses of DAT protein or changes in DAT surface levels, indicating that acute loss of palmitoylation leads to reduction of transport kinetics. Treatment of synaptosomes or cells with 2BP using higher doses or longer times resulted in DAT protein losses and production of transporter fragments, implicating palmitoylation in regulation of transporter degradation. Site-directed mutagenesis indicated that palmitoylation of rat DAT occurs at Cys-580 at the intracellular end of transmembrane domain 12 and at one or more additional unidentified site(s). Cys-580 mutation also led to production of transporter degradation fragments and to increased phorbol ester-induced down-regulation, further supporting palmitoylation in opposing DAT turnover and in opposing protein kinase C-mediated regulation. These results identify *S*-palmitoylation as a major regulator of DAT properties that could significantly impact acute and long term dopamine transport capacity.

In the central nervous system, dopamine (DA)[2] controls numerous processes, including motor activity, emotion, and reward; and many diseases, including Parkinson disease, depression, attention deficit hyperactivity disorder, and schizo-

phrenia, are related to abnormalities in dopaminergic function (1). The plasmalemmal dopamine transporter (DAT) actively transports DA from the extracellular space into the presynaptic neuron, and it is the primary mechanism controlling the concentration and duration of DA in the synapse (2). This activity is crucial for proper dopaminergic neurotransmission, and transport dysregulation is hypothesized to contribute to dopaminergic disorders (3). DAT is a major target for many abused and therapeutic drugs that inhibit transport or stimulate DA efflux (4, 5), leading to increased extracellular DA levels that induce psychomotor stimulation and drug addiction, or therapeutically modulate DA levels in mood and psychiatric disorders.

DAT is subject to extensive acute and chronic regulatory processes that modulate DA neurotransmission during momentary physiological demands and long term disease and drug addiction states (6, 7), but the mechanisms remain poorly understood. In model cell systems, regulation of transporter surface levels has been established as an element of acute control, as DAT surface levels are modulated by constitutive and regulated DAT endocytosis and membrane recycling (8–11). Activation of protein kinase C (PKC) stimulates endocytosis of transporters through early and late endosomes (9, 12–14) and ultimately into lysosomes where they are degraded (13, 15, 16). Several DAT N- and C-terminal domain motifs impact constitutive and regulated endocytosis and/or degradation (17–19), although the exact mechanisms of these processes are not yet known. DAT lateral membrane mobility, transport activity, and PKC-dependent down-regulation are also impacted through incompletely understood mechanisms that involve cholesterol (20, 21).

In the course of our DA transport regulation studies, we discovered that DAT undergoes *S*-palmitoylation, a post-translational modification in which C16-saturated palmitic acid is added via a thioester linkage to cysteine (22). Palmitoylation is reversible and dynamic, with addition and removal rapidly catalyzed by palmitoyl acyltransferases (PATs) and palmitoyl-protein thioesterases (PPTs), respectively. These modifications confer the ability of target proteins to respond to regulatory signals in a manner analogous to phosphorylation/dephosphorylation (22). *S*-Palmitoylation is known to control multiple functions of integral membrane proteins, including catalytic activity, trafficking, subcellular targeting, and turnover (23–25). In this study, we show that palmitoylation strongly influences DAT transport kinetics, degradation, and PKC-stimulated down-regulation, demonstrating the presence of previously unknown layers of control over the

[1] To whom correspondence should be addressed: Dept. of Biochemistry and Molecular Biology, University of North Dakota School of Medicine and Health Sciences, 501 N Columbia Rd., Stop 9037, Grand Forks, ND 58202-9037. Tel.: 701-772-6878; Fax: 701-777-2382; E-mail: rvaughan@medicine.nodak.edu.

[2] The abbreviations used are: DA, dopamine; LLC-PK, Lewis lung carcinoma-porcine kidney; 2BP, 2-bromopalmitic acid; PMA, phorbol 12-myristate 13-acetate; DAT, dopamine transporter; rDAT, rat DAT; hDAT, human DAT; SP, sucrose phosphate; MMTS, methyl methanethiosulfonate; ANOVA, analysis of variance; AMEM, α-minimum essential medium; Pal, palmitate; PPT, palmitoyl-protein thioesterase; PAT, palmitoyl acyltransferase; DiBAC$_4$(3), bis-(1,3-dibutylbarbituric acid)trimethine oxonol.

transporter and indicating the potential for this modification to be of prime importance in acute and long term regulation of DA neurotransmission.

EXPERIMENTAL PROCEDURES

Materials—[7,8-^{3}H]DA (45 Ci/mmol), L-[2,3-^{3}H]alanine (54 Ci/mmol), and high range Rainbow molecular mass standards were from GE Healthcare; [9,10-^{3}H]palmitic acid (73.4 Ci/mmol) and [9,10-^{3}H]myristic acid (60 Ci/mmol) were from Moravek; DA was from Research Biochemicals International; PMA was from Calbiochem; (−)-cocaine, Colorburst molecular mass standards, antibodies for tyrosine hydroxylase, α-tubulin, and polyhistidine, and other fine chemicals were from Sigma; FuGENE 6 transfection reagent and Complete Mini protease inhibitor tablets were from Roche Applied Bioscience; MMTS, (*N*-(6-(biotinamido)hexyl)-3′-(2′-pyridyldithio)-propionamide, sulfo-NHS-SS-biotin, high capacity NeutrAvidin-agarose resin, and bicinchoninic acid protein assay reagent were from Thermo Scientific; and DiBAC$_4$(3) was from Invitrogen. [^{125}I]RTI 82 was synthesized and radioiodinated as described previously (26). Rats were purchased from Charles River Laboratories, and SV129 mice were obtained from Dr. Eric Murphy, University of North Dakota. All animals were housed and treated in accordance with regulations established by the National Institutes of Health and approved by the University of North Dakota Institutional Animal Care and Use Committee.

Synaptosome Preparation—Male Sprague-Dawley rats (175–300 g) were decapitated, and striata were rapidly dissected, weighed, and placed in ice-cold sucrose phosphate (SP; 0.32 M sucrose and 10 mM sodium phosphate, pH 7.4) buffer. Tissue was homogenized in ice-cold SP buffer with 15 strokes in a glass/Teflon homogenizer and centrifuged at 3000 × g for 3 min at 4 °C, and the supernatant fraction was re-centrifuged at 17,000 × g for 12 min. The resulting P2 synaptosomal pellet was resuspended to 20 mg/ml original wet weight in ice-cold SP buffer and used for all synaptosomal studies except surface biotinylation analyses, which used purified synaptosomes (described below). Striatal synaptosomes from male SV129 mice were prepared using the same procedure.

Cell Culture and Mutagenesis—Lewis lung carcinoma-porcine kidney (LLC-PK$_1$) cells or LLC-PK$_1$ cells stably expressing the WT or mutant rat (r) dopamine transporter (rDAT-LLCPK$_1$) (27) were maintained in α-minimum essential medium (AMEM) supplemented with 5% fetal bovine serum, 2 mM L-glutamine, 200 μg/ml G418, and 100 μg/ml penicillin/streptomycin in a humidified incubation chamber gassed with 5% CO$_2$ at 37 °C. Mutant constructs with Cys residues 6, 135, 341, 522, and 580 changed to alanine were produced from the WT DAT cDNA using the Stratagene QuikChange® kit, with codon substitution verified by sequencing (Alpha Biolabs; Northwoods DNA). For production of stable transformants, LLC-PK$_1$ cells were grown to ∼50% confluency and transfected using FuGENE transfection reagent and 0.5 μg of the mutant rDAT pcDNA 3.0 plasmid. Transformants were selected 24–48 h later by the addition of 800 μg/ml geneticin

(G418) to the cell culture medium. His$_6$-hDAT HEK293 cells were maintained as described previously (28).

Metabolic Labeling of DAT with [^{3}H]Palmitate—P2 rat striatal synaptosomes were metabolically labeled with [9,10-^{3}H]palmitic acid (2 mCi/ml) for 90 min at 30 °C in HEPES-buffered DMEM. Cultured cells expressing WT or mutant DATs were metabolically labeled with [9,10-^{3}H]palmitic acid (0.5 mCi/ml) for 1–18 h at 37 °C in AMEM, which contained 1 mM sodium pyruvate to inhibit palmitate metabolism through fatty acid β-oxidation (29). For PAT inhibitor studies, labeling was performed in the presence of 1–15 μM 2-bromopalmitate (2BP) prepared in dimethyl sulfoxide (DMSO). After labeling, synaptosomes or cells were washed with SP buffer or phosphate-buffered saline, respectively, and lysed in radioimmunoprecipitation assay buffer (RIPA: 10 mM sodium phosphate, 150 mM NaCl, 2 mM EDTA, 50 mM sodium fluoride, 1% Triton X-100, 1% sodium deoxycholate, 0.1% SDS, pH 7.2).

Analysis of Palmitoylation by Acyl-Biotinyl Exchange—DAT palmitoylation was also assessed by acyl-biotinyl exchange (30, 31) using a method modified from Wan *et al.* (32). Briefly, synaptosomes were treated with vehicle or 2BP followed by centrifugation at 20,000 × g for 12 min at 4 °C. Synaptosomal pellets were solubilized in lysis buffer (50 mM HEPES, pH 7.0, 2% SDS, 1 mM EDTA) containing Mini Complete protease inhibitor and 20 mM MMTS to block free thiols. Lysates were incubated at ambient temperature for 1 h with mixing followed by acetone precipitation and resuspension in lysis buffer containing MMTS and incubation at ambient temperature overnight with end-over-end mixing. Excess MMTS was removed by three sequential acetone precipitations followed by resuspension of the precipitated proteins in 300 μl of a buffer containing 4% (w/v) SDS (4SB: 4% SDS, 50 mM Tris, 5 mM EDTA, pH 7.4). Each sample was divided into two equal portions (150 μl) that were treated for 2 h at ambient temperature with 50 mM Tris-HCl, pH 7.4, as control or 0.7 M hydroxylamine (NH$_2$OH), pH 7.4, to cleave the thioester bonds. NH$_2$OH was removed by three sequential acetone precipitations followed by resuspension of the precipitated proteins in 240 μl of 4SB buffer followed by dilution with 900 μl of 50 mM Tris-HCl, pH 7.4, containing 0.4 mM sulfhydryl-reactive (*N*-(6-(biotinamido)hexyl)-3′-(2′-pyridyldithio)-propionamide and incubation at ambient temperature for 1 h with end-over-end mixing. Unreacted (*N*-(6-(biotinamido)hexyl)-3′-(2′-pyridyldithio)-propionamide was removed by three sequential acetone precipitations followed by resuspension of the final pellet in 75 μl of lysis buffer without MMTS. Samples were diluted (1:20) with 50 mM Tris-HCl, pH 7.4, to contain 0.1% SDS, and biotinylated proteins in samples were affinity-purified using Neutravidin resin. Proteins were eluted with sample buffer (60 mM Tris, pH 6.8, 2% SDS, 10% glycerol) containing 100 mM dithiothreitol and 3% β-mercaptoethanol and subjected to SDS-PAGE and immunoblotting using anti-rat DAT monoclonal Ab16 (mAb16) (33).

Immunoprecipitation, Electrophoresis, and Autoradiography—Lysates of [^{3}H]palmitate-labeled tissue or cells were immunoblotted with mAb16 to determine DAT levels (33), and vol-

umes containing equal amounts of DAT (verified by second immunoblot) were immunoprecipitated with polyclonal Ab16 generated against rDAT N-terminal amino acids 42–59 (34). Precipitated DATs were resolved on 4–20% SDS-polyacrylamide gels using Rainbow molecular mass markers as standards, and gels were treated with Fluoro-Hance (Research Products International) fluorographic reagent for 30 min, dried, and exposed to x-ray film for 7–60 days. [3H]Palmitate band intensities were quantified using Quantity One® software (Bio-Rad), and values were normalized to the amount of DAT in samples determined by immunoblotting. For comparison across multiple experiments, [3H]palmitate labeling of mutant DAT was expressed as a fraction of the WT level normalized to 100%, and results were analyzed by Student's t test with significance set at $p < 0.05$. To verify the nature of the palmitate chemical linkage, protein A-Sepharose beads containing DAT immune complexes were treated with 1 M Tris-HCl, pH 7.4 (control), or 1 M NH_2OH, pH 7.4, for 2 h at 22 °C. All labeling results were replicated in 2–4 independent experiments.

[3H]DA and [3H]Alanine Uptake Assays—P2 rat striatal synaptosomes were treated with the indicated concentrations of palmitate (Pal) or 2BP prepared in DMSO for 60 min at 30 °C followed by [3H]DA or [3H]alanine uptake assay in modified Krebs phosphate buffer (126 mM NaCl, 4.8 mM KCl, 16 mM potassium phosphate, 1.4 mM $MgSO_4$, 10 mM glucose, 1.1 mM ascorbic acid, and 1.3 mM $CaCl_2$, pH 7.4) as described previously (35). Final DMSO was 1% or less, which by itself did not affect DA transport activity, and equal DMSO concentrations were used in all vehicle controls. Final concentrations of [3H]DA and [3H]alanine were 10 nM, and nonspecific uptake was determined by addition of 100 μM (−)-cocaine or 1 mM serine, respectively. For saturation analysis, synaptosomes were treated with vehicle or 5 μM 2BP prepared in DMSO for 45 min at 30 °C and assayed for DA uptake with unlabeled DA varying from 30 nM to 1 μM. For time course and PMA additivity studies, synaptosomes were treated with vehicle or 5 μM 2BP for the indicted times or by vehicle or 1 μM PMA for 30 min followed by [3H]DA transport assay. Uptake assays were performed in triplicate and were initiated by addition of synaptosomes to the reaction tube followed by incubation for 5 min at 30 °C. Uptake was stopped by addition of 5 ml of ice-cold SP buffer followed by immediate filtration using a Brandel tissue harvester through a Whatman GF/B filter soaked for 1 h in 0.1% BSA. Radioactivity retained on filters was assessed by liquid scintillation counting.

WT or C580A rDAT-LLCPK$_1$ cells grown in 24-well plates were treated with vehicle or 15 μM 2BP in AMEM for 18 h at 37 °C. Cells were rinsed twice with 0.5 ml of Krebs-Ringer/HEPES buffer (KRH: 25 mM HEPES, 125 mM NaCl, 4.8 mM KCl, 1.2 mM KH_2PO_4, 1.3 mM $CaCl_2$, 1.2 mM $MgSO_4$, 5.6 mM glucose, pH 7.4) followed by uptake assay. For PKC experiments, cells were incubated at 37 °C for 30 min with vehicle or 1 μM PMA followed by [3H]DA transport assay. Uptake was performed in triplicate and initiated by addition of 10 nM [3H]DA plus 3 μM DA except for saturation analyses where unlabeled DA varied from 0.3 to 30 μM. Nonspecific uptake was determined in the presence of 100 μM (−)-cocaine. Up-

take was allowed to proceed for 8 min, and cells were rapidly washed three times with ice-cold KRH. Cells were then solubilized in 1% Triton X-100, and radioactivity contained in lysates was assessed by liquid scintillation counting.

Synaptosomal Surface Biotinylation—For surface biotinylation studies, purified synaptosomes were isolated using the discontinuous Percoll gradient method of Dunkley *et al.* (36). The P2 crude synaptosomal pellet prepared as described above was resuspended in 2 ml of SP buffer and layered on top of a discontinuous gradient containing 2-ml layers of 3, 10, 15, and 23% Percoll in SP buffer. Gradients were centrifuged at $31,000 \times g$ for 7 min at 4 °C in a Beckman JA-25 rotor, and purified synaptosomes were recovered from the 15–23% interface. Synaptosomes were washed by addition of 20 volumes of SP buffer followed by centrifugation at $17,000 \times g$ for 12 min and resuspension of the pellet in 3.6 ml of SP buffer. Purified synaptosomes were treated with vehicle, 1 μM PMA, or 10 μM 2BP at 30 °C for 30 min, and aliquots were assayed for [3H]DA transport activity or were transferred to an ice bath and incubated at 4 °C for 25 min with the membrane-impermeable biotinylating reagent sulfo-NHS-SS-biotin (1.5 mg/ml). Biotinylated synaptosomes were centrifuged at $17,000 \times g$ for 12 min at 4 °C, resuspended in SP buffer, and given a second incubation with sulfo-NHS-SS-biotin (1.5 mg/ml). Synaptosomes were centrifuged at $17,000 \times g$ for 12 min at 4 °C, resuspended in SP buffer containing 100 mM glycine, pH 7.4, for 30 min at 4 °C, recentrifuged at $17,000 \times g$ for 12 min at 4 °C, and solubilized with 300 μl of RIPA buffer. Biotinylated DATs were isolated by NeutrAvidin-Sepharose chromatography, separated by SDS-PAGE, and quantified by immunoblotting with mAb16 as described previously (21). Total lysate and biotinylated fractions were immunoblotted for the cytoplasmic enzyme tyrosine hydroxylase as a control for dopaminergic membrane integrity.

RESULTS

Identification of DAT Palmitoylation—LLCPK$_1$ cells stably transfected with wild type (WT) rDAT were metabolically labeled with 10 μM [3H]palmitic acid for 1–18 h, and DATs were extracted by immunoprecipitation and subjected to SDS-PAGE/fluorography. In initial studies, [125I]RTI 82 photoaffinity-labeled DATs (37) were immunoprecipitated and electrophoresed in parallel to confirm electrophoretic migration of bands. A [3H]palmitate-labeled band that co-migrated with [125I]RTI 82-labeled DAT was observed at the DAT monomeric mass of ~100 kDa (Fig. 1*A*), and it was not seen in samples precipitated with preimmune serum or from LLCPK$_1$ cells, verifying its identity as DAT. Analogous studies were performed with native DAT by labeling rat striatal synaptosomes with 40 μM [3H]palmitic acid for 90 min. Again we obtained an ~100-kDa band that precipitated with immune but not preimmune DAT antiserum (Fig. 1*B*). To characterize the nature of the radioactive label, we treated the precipitated protein with hydroxylamine (NH_2OH), which chemically cleaves fatty acylated thioester bonds (38). This released >80% of the radiolabel from both expressed and native DATs (Fig. 1, *A* and *B*), demonstrating the thioacyl nature of the bond. Time course studies in cells showed that [3H]palmitate
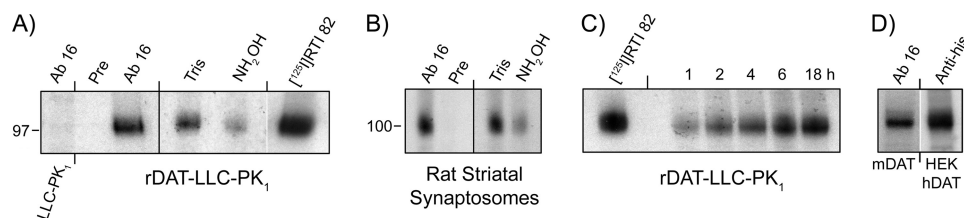
FIGURE 1. **S-Palmitoylation of DAT.** rDAT-LLCPK$_1$ cells (*A*) and rat striatal synaptosomes (*B*) were metabolically labeled with [^{3}H]palmitic acid for 18 h or 90 min, respectively, and lysates were precipitated with Ab16 followed by SDS-PAGE/fluorography. Preimmune antiserum (*pre*) and LLCPK$_1$ cells served as negative controls, and migration of bands was verified by parallel electrophoresis of [^{125}I]RTI 82-labeled DAT. For acyl thioester analyses, precipitates from cells or synaptosomes were treated with Tris-HCl or hydroxylamine (*NH$_2$OH*) as indicated. *C*, rDAT-LLCPK$_1$ cells were incubated with [^{3}H]palmitate for the indicated times followed by immunoprecipitation and SDS-PAGE/fluorography of DAT. *D*, mouse striatal synaptosomes and His$_6$-hDAT HEK 293 cells were labeled with [^{3}H]palmitate for 90 min or 18 h, respectively, and DATs were precipitated with Ab16 or anti-His antibodies followed by SDS-PAGE/fluorography. Results are representative of three or more independent experiments.
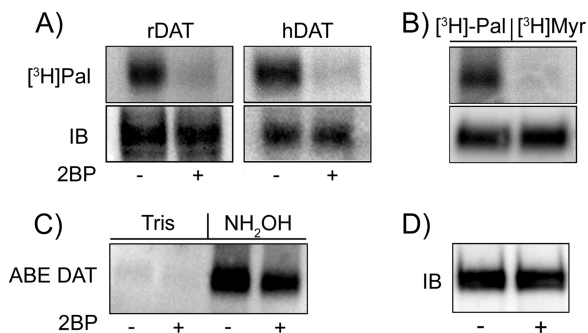

FIGURE 2. **DAT palmitoylation specificity and inhibition by 2BP.** *A*, rDAT-LLCPK$_1$ cells or His$_6$-hDAT-HEK 293 cells were labeled for 18 h with 10 μM [^{3}H]palmitate in the presence or absence of 15 μM 2BP. *B*, rat striatal synaptosomes were labeled with 40 μM [^{3}H]palmitic acid or 40 μM [^{3}H]myristic acid (*Myr*) for 90 min. Equal amounts of DAT were immunoprecipitated and analyzed by SDS-PAGE/fluorography ([^{3}H]pal) or immunoblotting (*IB*). *C*, rat striatal synaptosomes were treated with 5 μM 2BP for 45 min at 30 °C followed by acyl-biotinyl exchange (*ABE*). Samples were treated with Tris-HCl, pH 7.4 (control), or NH$_2$OH to remove thioester-linked palmitate, followed by sulfhydryl-reactive biotinylation, NeutrAvidin extraction, and DAT immunoblotting. *D*, DAT immunoblot of vehicle and 2BP-treated samples. All results are representative of three or more independent experiments.

labeling of DAT occurred within 60 min (Fig. 1*C*), indicative of rapid palmitate turnover, and increased steadily up to 18 h. We also demonstrated [^{3}H]palmitate labeling of DAT from mouse striatal synaptosomes and His$_6$-hDAT expressed in HEK 293 cells (Fig. 1*D*), verifying palmitoylation of these species homologs.

To evaluate further the nature of the modification, we treated cells with 2BP, which irreversibly inhibits all PAT enzymes and is widely used to analyze palmitoylation functions (39). Treatment of rDAT-LLCPK$_1$ cells and hDAT-HEK 293 cells with 15 μM 2BP inhibited [^{3}H]palmitate labeling of both forms of DAT by >80% (Fig. 2*A*). We also found that rat striatal DAT was not labeled with the C14-saturated lipid [^{3}H]myristic acid under conditions positive for [^{3}H]palmitate labeling (Fig. 2*B*) demonstrating the specificity of labeling. Because of the limitations imposed by the short [^{3}H]palmitate labeling times possible in rat striatal synaptosomes, we assessed 2BP effects on striatal DAT palmitoylation using the acyl-biotinyl exchange method (30–32), in which endogenous acyl thioesters are removed by NH$_2$OH and replaced *in vitro* with a sulfhydryl-specific biotinylating reagent. Using this method, we found that treatment of synaptosomes with 5 μM 2BP for 45 min decreased the DAT palmitoylation level to 64 $\pm$ 3% of control (*p* < 0.001 by ANOVA with Dunnett's

post test, *n* = 3) (Fig. 2*C*). Control samples pretreated with Tris displayed negligible incorporation of the sulfhydryl reagent, demonstrating the specificity of labeling for sites modified *in vivo* and immunoblotting showed that DAT levels were not changed by the 2BP treatment (Fig. 2*D*). Together, these results demonstrate that 2BP suppresses palmitoylation of both native and heterologously expressed DATs.

2BP Effects on Rat Striatal DAT—The effective inhibition of DAT palmitoylation with 2BP allowed us to use this treatment to investigate the impact of acute modulation of palmitoylation on transporter functions. For studies in brain tissue, we treated rat striatal synaptosomes with 2BP, using vehicle or equal concentrations of palmitate (Pal) as negative controls (Fig. 3). Neither total protein (data not shown) nor α-tubulin immunoreactivity (Fig. 3*B*) was affected by the treatments, indicating that these conditions do not cause obvious toxicity.

Fig. 3*A* shows [^{3}H]DA transport activity from rat striatal synaptosomes treated for 60 min with vehicle or 1–10 μM Pal or 2BP. Transport activity in synaptosomes given Pal treatments showed modest decreases that reached statistical significance from vehicle controls at 10 μM palmitate (70 $\pm$ 8% of control, *p* < 0.05). In contrast, 2BP caused a highly significant effect, with a trend toward decreased [^{3}H]DA transport (73 $\pm$ 9% of control) produced by 1 μM 2BP and transport reductions to 44 $\pm$ 5 and 31 $\pm$ 3% of vehicle control produced by 5 and 10 μM 2BP, respectively (both *p* < 0.001 relative to vehicle and *p* < 0.01 relative to Pal). Immunoblotting of lysates from these samples (Fig. 3*B*) showed that DAT levels were not changed by any of the Pal treatments or by 1 or 5 μM 2BP but were reduced to 76 $\pm$ 4% of control by 10 μM 2BP (*p* < 0.05 relative to vehicle). Thus, the ~50% transport reduction caused by 5 μM 2BP occurred with no detectable loss of DAT protein, and the ~70% DA transport reduction caused by 10 μM 2BP was accompanied by an ~25% loss of DAT protein. These results indicate that acute suppression of DAT palmitoylation by lower concentrations of 2BP (5 μM) leads to a reduction in DA transport capacity that occurs without changes in transporter levels, whereas higher concentrations of 2BP (10 μM) induce a loss of DAT protein that correlates with further transport reductions.

To determine whether the reduction in DA transport activity induced by 2BP could be caused by effects on electrochemical gradients needed to drive transport, aliquots of the synaptosomes used in three of the DA transport analyses in Fig. 3*A* were assayed in parallel for Na$^+$-dependent [^{3}H]alanine up-
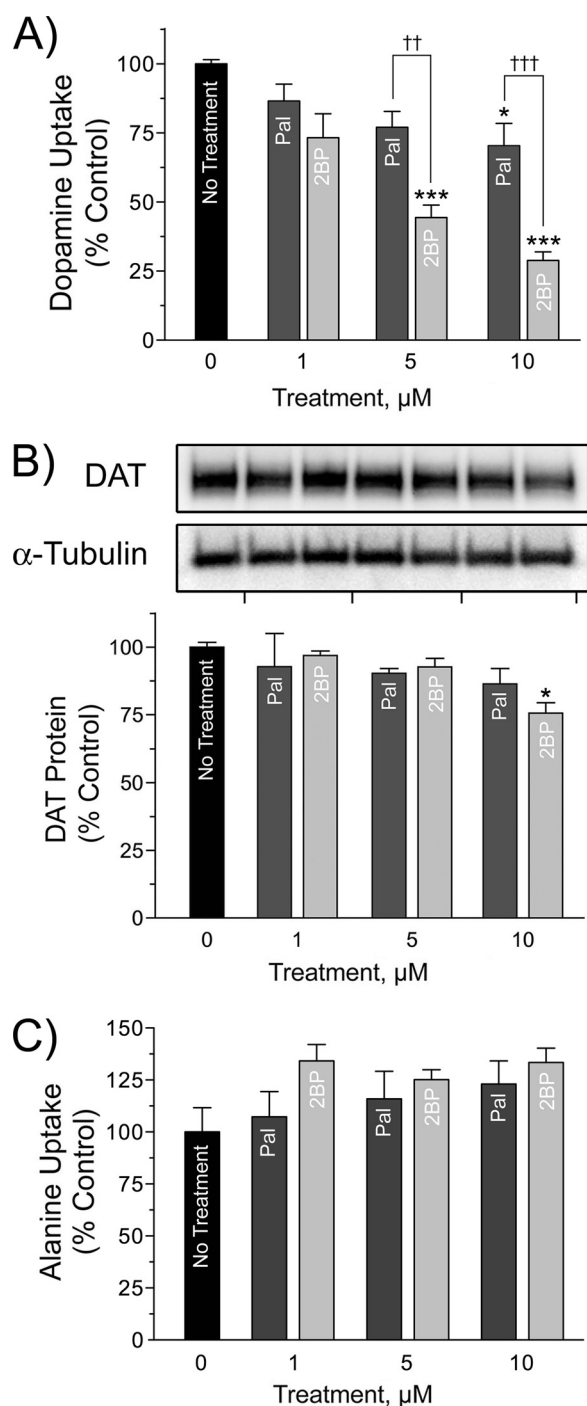
A)

B)

C)

FIGURE 3. 2BP reduces DA transport activity and DAT levels in rat striatal synaptosomes. Rat striatal synaptosomes were treated with vehicle (no treatment) or the indicated concentrations of palmitate (*Pal*) or 2BP at 30 °C for 60 min, and aliquots were analyzed for [³H]DA transport, [³H]alanine transport, or DAT immunoblotting. *A,* [³H]DA transport activity (means ± S.E. of 3–4 experiments performed in triplicate) relative to vehicle controls normalized to 100%. *, $p < 0.05$; ***, $p < 0.001$, 2BP or Pal *versus* vehicle; ††, $p < 0.01$, †††, $p < 0.001$ 2BP *versus* Pal (one-way ANOVA with Tukey's post test). *B,* equal amounts of protein from treated synaptosomes (conditions indicated directly below on histogram) were immunoblotted for DAT (representative blot shown), and band density was expressed as a fraction of control values normalized to 100% (means ± S.E. of three experiments performed in duplicate). *, $p < 0.05$, 2BP *versus* vehicle control (one-way ANOVA with Tukey's post test). DAT blots were stripped and re-probed for α-tubulin, which showed no change with Pal or 2BP treatment. *C,* [³H]alanine transport activity (means ± S.E. of three experiments performed in triplicate) relative to controls normalized to 100%.
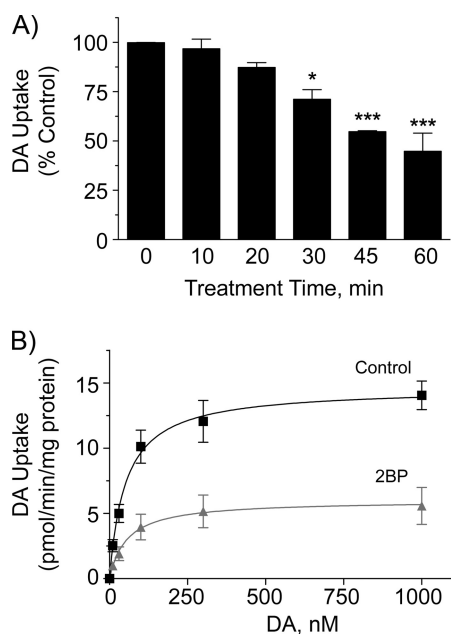
A)

B)

FIGURE 4. Kinetic analysis of 2BP effects in synaptosomes. *A,* rat striatal synaptosomes were treated for the indicated times with vehicle or 5 μM 2BP at 30 °C followed by [³H]DA transport assay. Transport values obtained with 2BP treatment are calculated as the fraction of activity relative to each time point control. Values shown are means ± S.E. of three experiments performed in triplicate; *, $p < 0.05$; ***, $p < 0.001$ relative to time point control (one-way ANOVA with Tukey's post test). *B,* saturation analysis of rat striatal synaptosomes treated with vehicle or 5 μM 2BP for 45 min. Results shown are means ± S.E. of three independent experiments performed in triplicate.

take (40). Alanine transport was not statistically different from vehicle or palmitate controls at any of the 2BP concentrations (Fig. 3*C*), demonstrating that the treatment did not induce global effects capable of reducing Na^+-dependent solute transport. We also examined the electrochemical potential of synaptosomes using the anionic lipophilic dye $DiBAC_4(3)$, which undergoes increased fluorescence with membrane depolarization (41, 42). Synaptosomes treated with vehicle or 2BP were incubated with $DiBAC_4(3)$, and fluorescence was measured as described previously (33). Base-line $DiBAC_4(3)$ fluorescence of synaptosomes was not affected by treatment with 10 μM 2BP for 30, 60, or 90 min, and all control and treated synaptosomes showed equal fluorescence increases with K^+-induced depolarization (data not shown), further supporting a lack of 2BP effect on electrochemical gradients needed to drive transport.

The time course of 2BP effects on uptake in rat striatal synaptosomes is shown in Fig. 4*A*. Treatment of synaptosomes with 5 μM 2BP caused no significant effect on transport activity during the first 10 or 20 min of treatment (97 ± 5 and 87 ± 3% of control, respectively), indicating that 2BP is not a direct DA uptake inhibitor. Cocaine inhibition of uptake in synaptosomes was also unaffected by 2BP (data not shown) further supporting a lack of direct effect on transporter active sites. By 30, 45, and 60 min of treatment, transport was reduced 71 ± 5, 55 ± 1, and 45 ± 9 of control ($p < 0.05$ and $p < 0.001$), with no differences in DAT protein levels between control and 2BP samples at any time point (data not shown). This time course is consistent with that of 2BP inhibition of DAT palmitoylation (Fig. 2*C*) and with the time dependence
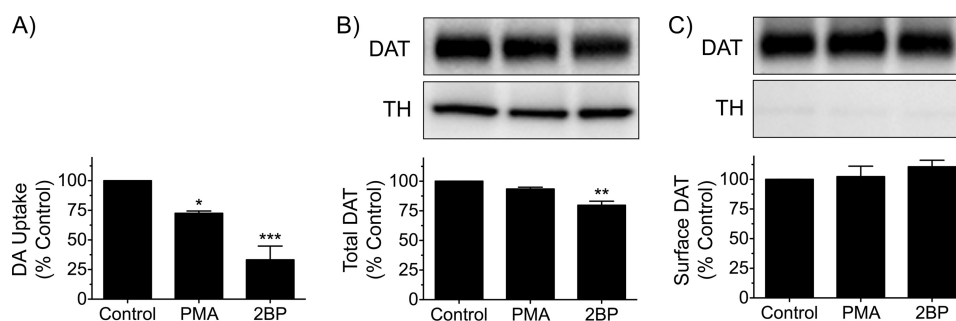
FIGURE 5. **Surface biotinylation analysis of 2BP-treated synaptosomes.** Percoll gradient-purified synaptosomes were treated with vehicle, 1 μM PMA, or 7.5 μM 2BP for 30 min at 30 °C, and aliquots were assayed for [^{3}H]DA transport activity or subjected to surface biotinylation. All results shown are means ± S.E. of three independent experiments performed in triplicate. *A,* [^{3}H]DA transport activity of synaptosomes normalized to vehicle controls; *, $p < 0.05$; ***, $p < 0.001$; relative to control by ANOVA with Dunnett's post test. *B,* equal amounts of protein from control and treated synaptosomes were immunoblotted for DAT or tyrosine hydroxylase (*TH*). *Upper panel* shows representative immunoblots (*lanes* correspond to treatments shown directly below on histogram). *Histogram* shows quantification of DAT levels, **, $p < 0.01$ relative to control by ANOVA with Dunnett's post test. *C,* fractions eluted from NeutrAvidin resin were immunoblotted for DAT and tyrosine hydroxylase (*upper panels*). *Histogram* shows quantification of biotinylated DAT normalized for total DAT protein, $p > 0.05$ by ANOVA with Dunnett's post test.

of PAT inhibition by 2BP (39). Saturation analysis of synaptosomes treated with 5 μM 2BP for 45 min (Fig. 4*B*) showed that V_{max} was significantly reduced relative to control (7.2 ± 1.7 *versus* 16.0 ± 0.5 pmol/min/mg, $p < 0.05$), whereas the K_m value for DA was not affected (50.3 ± 16.4 *versus* 47.5 ± 1.6 nM, $p > 0.05$). Immunoblotting confirmed no loss of DAT protein by the treatment (2BP samples 96 ± 6% of control, $p > 0.05$).

To probe the mechanism of 2BP-induced transport reduction in synaptosomes, we performed surface biotinylation analysis. In initial studies, we used P2 synaptosomes for these experiments but found that the negative biotinylation control (the cytosolic enzyme tyrosine hydroxylase) for assessment of membrane integrity consistently showed strongly positive biotinylation signals. Therefore, for this analysis, we found it necessary to use Percoll gradient-purified synaptosomes, which produced valid negative biotinylation control results. The synaptosomes were treated for 30 min with vehicle, 7.5 μM 2BP, or 1 μM PMA, and aliquots were assayed for [^{3}H]DA transport or subjected to surface biotinylation analysis. In three independent experiments performed in triplicate (Fig. 5*A*), we found that DA transport activity was reduced to 73 ± 2% of control by PMA and to 33 ± 12% of control by 2BP (both $p < 0.001$). Total DAT values were not changed with PMA and were slightly reduced with 2BP treatment (80 ± 3% of control, $p < 0.01$) (Fig. 5*B*). Thus, compared with the P2 synaptosomes used in other experiments, the purified synaptosomes showed slightly increased sensitivity to 2BP-induced transport down-regulation and DAT protein losses. Quantification of biotinylated forms for each treatment showed surface levels of DAT were not different from control levels when normalized for total transporter protein (PMA, 102 ± 9% of control; 2BP, 111 ± 5% of control, both $p > 0.05$) (Fig. 5*C*), with 12.3 ± 2.1% of transporters in control synaptosomes biotinylated. The integrity of the synaptosome plasma membranes to the biotinylating reagent was demonstrated by immunoblotting of the dopaminergic cytosolic enzyme tyrosine hydroxylase, which showed strong staining in total samples (Fig. 5*B*) and negligible staining (<3% of total) in biotinylated fractions (Fig. 5*C*). These results indicate that the reductions of transport activity induced by PMA and 2BP beyond that

consistent with transporter loss are not accompanied by reduced DAT plasma membrane levels, supporting an alteration of transport kinetic processes as the mechanism of transport reduction for both conditions.

Mutation of the DAT Palmitoylation Site—To determine which residue(s) of rDAT are palmitoylated, we made Cys → Ala mutations of all intracellularly oriented cysteines (Cys-6, Cys-135, Cys-341, Cys-522, and Cys-580) (Fig. 6*A*) and stably expressed the proteins in LLCPK$_1$ cells. All proteins were synthesized as determined by immunoblotting, with mutants expressed at 25–60% of WT levels relative to total protein. For palmitoylation analysis, cells expressing WT or mutant DATs were labeled in parallel with [^{3}H]palmitate, and equal amounts of DAT were immunoprecipitated and analyzed by SDS-PAGE/fluorography and immunoblotting (Fig. 6*B*, *upper* and *middle panels*). Quantification of [^{3}H]palmitate band intensities normalized to DAT protein showed palmitoylation levels of 100 ± 11% for WT DAT, 133 ± 4% for C6A DAT, 85 ± 35% for C135A DAT, 192 ± 44% for C341A DAT, and 85 ± 40% for C522A DAT, none of which were statistically different from WT DAT, whereas labeling of C580A DAT was reduced to 41 ± 11% of the WT DAT level ($p < 0.05$) (Fig. 6*C*). The [^{3}H]palmitate signal remaining on C580A DAT was specific as determined by comparison of samples precipitated with immune and preimmune serum (Fig. 6*B*, *lower panel*), demonstrating the presence of significant levels of palmitoylation on one or more additional currently unknown site(s).

We examined several properties of C580A and other DAT Cys → Ala mutants to determine the effects of loss of palmitoylation. All forms expressed fully mature glycosylated protein, and the ratios of mature and nonglycosylated immature forms were not different from the WT transporter (Fig. 6*B*, *middle panel*), indicating that the mutations did not prevent progress through the biosynthetic pathway. Little to no [^{3}H]palmitate labeling could be seen in the immature forms, although the low levels of these forms in conjunction with the low signal strength of the radiolabel makes this assessment difficult. All Cys → Ala mutants possessed cocaine-displaceable [^{3}H]DA transport activity that was roughly proportional to their overall expression level (data not shown), and surface biotinylation analysis showed no differences in steady-state
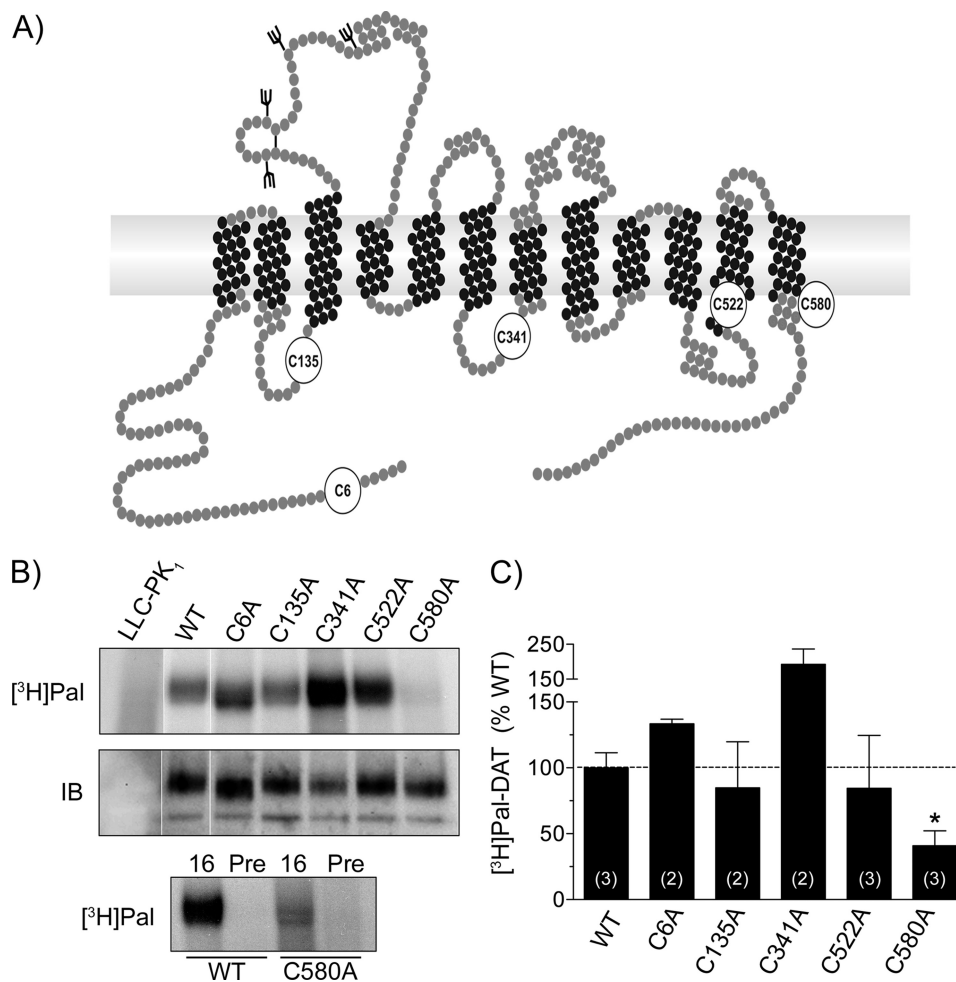
FIGURE 6. **Reduction of rDAT palmitoylation by C580A mutation.** *A,* diagram of rDAT modeled as in Beuming *et al.* (49) highlighting Cys residues analyzed in this study (*numbered circles*). *B,* LLCPK$_1$ cells stably expressing WT or Cys → Ala rDATs were labeled with [^{3}H]palmitate, and equal amounts of DAT were immunoprecipitated with Ab16 followed by SDS-PAGE/fluorography (*top panel*) or were immunoblotted (*middle panel*). LLCPK$_1$ cells were labeled in parallel, and lysate amounts equal to that used for WT DAT were analyzed as negative controls. *Bottom panel,* equal amounts of WT and C580A DAT were precipitated with immune (16) or preimmune (*pre*) antiserum followed by SDS-PAGE/auto fluorography. *IB,* immunoblot. *C,* quantification of DAT [^{3}H]palmitate labeling relative to DAT protein levels (means ± S.E. of 2–3 experiments as indicated performed in duplicate). *, $p < 0.05$ relative to WT, student's *t* test.

fraction of WT and C580A DATs at the plasma membrane when normalized to total transporter levels (C580A DAT surface level 98 ± 4% of WT DAT surface level, $p > 0.05$, $n = 3$). Saturation analysis showed no difference in DA K_m values for C580A and WT DATs (1.5 ± 0.2 and 1.4 ± 0.2 μM, respectively, $p > 0.05$, $n = 3$), whereas C580A DAT V_{max} was lower than of WT DAT (256 ± 13 *versus* 642 ± 22 pmol/min/mg, respectively, $p < 0.05$, $n = 3$) in rough proportion to transporter levels determined by immunoblotting (C580A DAT levels 32 ± 4% of WT DAT). Potencies for cocaine inhibition of [^{3}H]DA transport were not different between C580A and WT DATs (IC$_{50}$, 1.1 ± 0.1 and 1.1 ± 0.2 μM, respectively, $p > 0.05$, $n = 3$). These results indicate that C580A mutation does not significantly affect DAT steady-state surface levels or transport kinetic parameters.

2BP Effects on Heterologously Expressed DAT—2BP also caused pronounced effects on DATs expressed heterologously in LLC-PK$_1$ cells, although significant differences from synaptosome results were seen. Dose and time course studies in these cells showed that transport inhibition required higher

doses of 2BP (15–25 μM) and longer treatment times (2–18 h) than needed for synaptosomes, with only 5–10% transport reductions seen by 1–2 h of treatment (data not shown). Treatment of rDAT-LLCPK$_1$ cells with 15 μM 2BP for 18 h (Fig. 7*A*) led to reduction of both DA transport activity (78 ± 4% of control, $p < 0.001$) and DAT protein (52 ± 3% of control, $p < 0.001$). A similar pattern was seen in hDAT-HEK293 cells (data not shown), indicating that human DATs also respond to these treatments. Neither total protein nor α-tubulin immunoreactivity was affected by these treatments (data not shown), indicating that DAT protein losses did not occur due to global effects on protein stability. Saturation analysis (Fig. 7*B*) showed that 2BP-induced transport reductions occurred via reduced V_{max} (2BP, 1571 ± 106 pmol/min/mg; control, 1950 ± 79 pmol/min/mg; $p < 0.05$), with no effect on K_m values (2BP, 1.9 ± 0.3 μM; control 2.4 ± 0.5 μM; $p > 0.05$), with immunoblotting verifying reduction of DAT levels to 69 ± 13% of control ($p < 0.05$). Thus, in rDAT-LLCPK$_1$ cells, the rapid component of 2BP-induced down-regulation seen in synaptosomes that occurred with no loss of DAT protein was
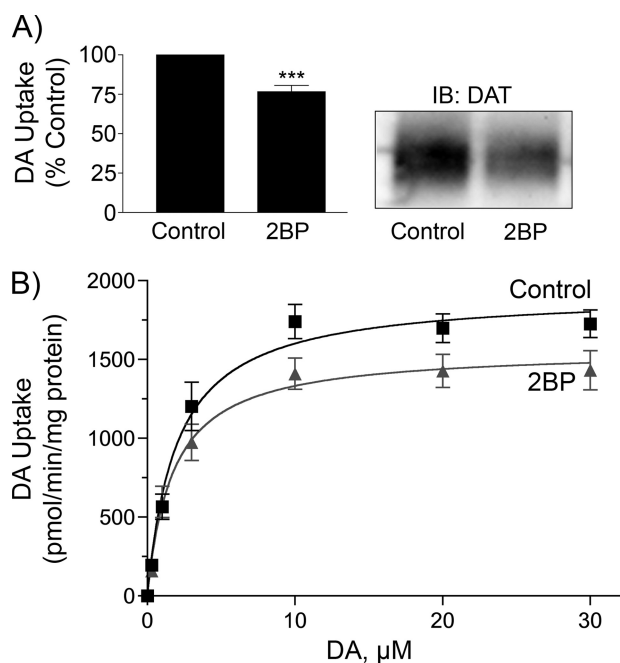
A)

B)

FIGURE 7. 2BP effects on DA transport and DAT levels in heterologous cells. *A,* rDAT-LLCPK$_1$ cells were treated with vehicle or 15 μM 2BP for 18 h followed by [^{3}H]DA transport assay or immunoblotting of equal amounts of protein for DAT. *Left, histogram* shows transport activity (means $\pm$ S.E. of four independent experiments performed in triplicate). ***, *p* < 0.001, 2BP *versus* control (one-way ANOVA with Dunnett's post test). *Right,* representative immunoblot of DAT from control and 2BP-treated cells. *B,* saturation analysis rDAT-LLCPK$_1$ cells treated with or without 15 μM 2BP for 18 h. Results shown are means $\pm$ S.E. of six independent experiments.
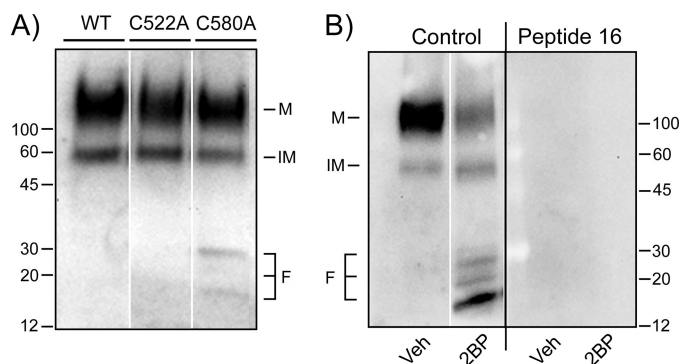
A) B)

FIGURE 8. Enhancement of DAT losses and degradation fragment production with C580A mutation and 2BP treatment. *A,* equal amounts of DAT from WT, C522A, or C580A rDAT-LLCPK$_1$ cell lysates were immunoblotted with MAb16. Markers indicate mature glycosylated protein (*M*), immature nonglycosylated protein (*IM*), and fragments (*F*). *B,* equal amounts of protein from C580A DAT-LLCPK$_1$ cells treated with vehicle (*Veh*) or 15 μM 2BP for 18 h were immunoblotted for DAT using control or peptide 16 preabsorbed antiserum.

not strongly present, and the magnitude of DAT protein loss was sufficient to explain the reduction of transport activity.

Inhibition of Palmitoylation Increases DAT Degradation— The 2BP-induced reduction of DAT protein at higher doses and/or longer treatment times in both synaptosomes and cells suggests that extensive suppression of DAT palmitoylation enhances transporter degradation. Consistent with this idea, we found that Western blots of C580A rDAT-LLCPK$_1$ cell lysates frequently contained multiple low molecular weight mAb16-immunoreactive peptides (Fig. 8*A*) that are likely to represent DAT degradation products, as their masses (15–30

kDa) are considerably lower than that of nascent DAT, which migrates at ~60 kDa. These fragments were not seen in lysates from WT or C522A DAT cells (Fig. 8*A*) or from cells expressing C135A, C242A, or C341A DATs (data not shown), supporting their origination from C580A DAT. Treatment of C580A rDAT-LLCPK$_1$ cells with 2BP dramatically increased the level of these fragments in conjunction with pronounced loss of full-length DAT (Fig. 8*B, left*), consistent with a precursor-product relationship. Preabsorption of mAb16 with its immunogenic peptide completely blocked staining of mature and immature full-length DAT protein and all low molecular weight bands (Fig. 8*B, right panel*), demonstrating the specificity of fragment immunoreactivity.

Because PKC has been shown in multiple studies to increase the rate of DAT degradation (13, 16, 18), we investigated the potential interaction between palmitoylation-related and PKC-stimulated DAT degradation. For these experiments, WT and C580A rDAT-LLCPK$_1$ cells were treated with vehicle or 15 μM 2BP for 18 h, with vehicle or PMA added for the final 30 min, and DATs were analyzed by immunoblotting (Fig. 9*A*), normalizing WT and C580A sets to contain equivalent levels of control DAT protein. Quantification of full-length mature DAT for each treatment relative to its control is shown in Fig. 9*B*. In cells treated with 2BP, WT DAT protein was reduced to 52 $\pm$ 3% of control (*p* < 0.001), whereas C580A DAT protein was reduced to 30 $\pm$ 5% of control (*p* < 0.001). The reduction of C580A DAT protein by 2BP was significantly greater than that of the WT protein (*p* < 0.001 relative to WT 2BP treatment level), and it was accompanied by marked increases in production of degradation fragments (Fig. 9*A, right two lanes*), indicating that Cys-580 mutagenesis and 2BP together impact DAT degradation more strongly than each condition separately. In addition, whereas PMA alone had no detectable effect on WT DAT levels or appearance of fragments under either control or 2BP conditions (Fig. 9, *A* and *B*), it caused a statistically significant decrease of full-length C580A DAT protein (83 $\pm$ 6% of control, *p* < 0.05), indicating that C580A DATs possess increased sensitivity to PKC-stimulated degradation.

Effects of Palmitoylation on DAT Regulation by PKC—We also determined the effects of 2BP on PKC-dependent regulation of DA transport activity in rat striatal synaptosomes and in WT and C580A rDAT-LLCPK$_1$ cells (Fig. 10). For striatal tissue experiments (Fig. 10*A*), synaptosomes were treated with 1 μM PMA or 5 μM 2BP separately or together for 30 min prior to transport assay. Western blotting showed no changes in DAT protein for any condition (data not shown). DA transport activity was reduced to 69 $\pm$ 2% of control by PMA (*p* < 0.001), to 65 $\pm$ 4% of control by 2BP (*p* < 0.001), and to 47 $\pm$ 3% of control by combined PMA and 2BP treatments (*p* < 0.001 relative to control; *p* < 0.001 or *p* < 0.01 relative to individual treatments), demonstrating additivity of PMA and 2BP effects.

For analysis of combination treatments in cells, WT or C580A rDAT-LLCPK$_1$ cells were treated with vehicle or 15 μM 2BP for 18 h followed by vehicle or 1 μM 2PMA for the final 30 min prior to transport assay (Fig. 10*B*). For WT DAT, transport activity was reduced to 70 $\pm$ 4% of control by PMA
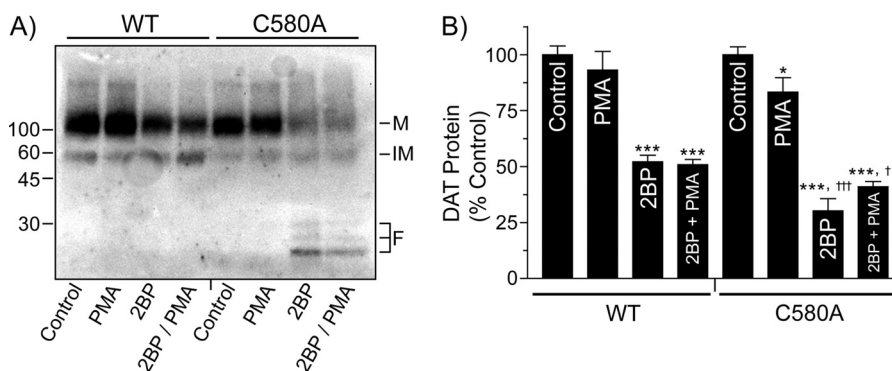
FIGURE 9. **2BP and PMA effects on WT and C580A DAT levels.** *A,* cells expressing WT or C580A DATs were treated with vehicle or 15 μM 2BP for 18 h followed by vehicle or 1 μM PMA for the final 30 min. Lysates were immunoblotted for DAT, and markers indicate mature (*M*) and immature (*IM*) DAT forms and fragments (*F*). *B,* quantification of full-length DAT from each treatment (means $\pm$ S.E. of four independent experiments). *, $p < 0.05$; ***, $p < 0.001$, indicated treatments *versus* control; †, $p < 0.05$; †††, $p < 0.001$, C580A *versus* WT for indicated treatments (one-way ANOVA with Tukey's post test).
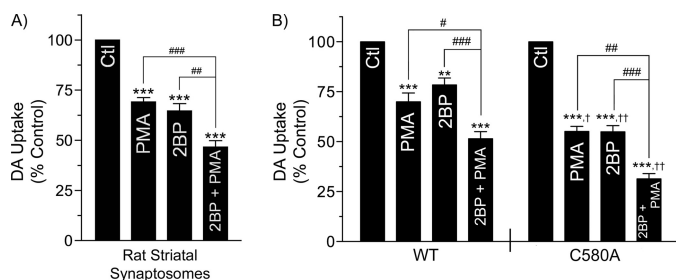

FIGURE 10. **Additivity of PMA, 2BP, and C580A effects on DA transport activity.** *A,* rat striatal synaptosomes were treated with the indicated combinations of 5 μM 2BP and 1 μM PMA for 30 min followed by assay for [³H]DA transport. Results shown are means $\pm$ S.E. of four independent experiments performed in triplicate. ***, $p < 0.001$ indicated treatments *versus* control; ##, $p < 0.05$; ###, $p < 0.001$; 2BP plus PMA *versus* 2BP or PMA only (one-way ANOVA with Tukey's post hoc test). *Ctl,* control. *B,* cells expressing WT or C580A DATs were treated with vehicle or 15 μM 2BP for 18 h followed by vehicle or 1 μM PMA for the final 30 min prior to [³H]DA transport assay. Results shown are means $\pm$ S.E. of 3–5 independent experiments performed in triplicate. **, $p < 0.01$; ***, $p < 0.001$ indicated treatments *versus* control; #, $p < 0.05$; ##, $p < 0.01$; ###, $p < 0.001$, WT or C580A DATs, PMA plus 2BP *versus* PMA, or 2BP only; †, $p < 0.05$; ††, $p < 0.01$, C580A *versus* WT DATs for indicated treatment groups (one-way ANOVA with Tukey's post hoc test).

($p < 0.001$), to 78 $\pm$ 4% of control by 2BP ($p < 0.01$), and to 52 $\pm$ 4% of control by PMA plus 2BP ($p < 0.001$ relative to control; $p < 0.05$ or $p < 0.001$ relative to individual treatments), again showing additivity of effects. The same pattern was seen in hDAT-HEK 293 cells (data not shown). For C580A DATs, transport activity was reduced to 55 $\pm$ 3% by PMA ($p < 0.001$), to 55 $\pm$ 3% by 2BP ($p < 0.001$), and to 31 $\pm$ 3% by PMA plus 2BP ($p < 0.001$ relative to control; $p < 0.01$ or $p < 0.001$ relative to individual treatments), also showing additivity of effects. For each treatment condition, C580A DAT showed statistically greater transport reductions than WT DAT (PMA $p < 0.05$; 2BP $p < 0.01$; PMA plus 2BP $p < 0.01$; C580A DAT relative to WT DAT). The greater extent of 2BP-induced down-regulation for C580A DAT compared with WT DAT indicates that suppression of palmitoylation by mutagenesis and 2BP together impacts transport activity more strongly than each condition separately. In addition, the increased level of PMA-induced down-regulation of C580A DAT relative to the WT transporter suggests that depalmitoylated DATs are more sensitive than palmitoylated DATs to PKC-induced transport down-regulation.

DISCUSSION

In this study, we demonstrate that DAT undergoes thioacylation with palmitic acid and show that this modification exerts multiple layers of control over the protein via impacts on transport capacity, degradation, and PKC-dependent regulation. Our findings reveal a distinction between 2BP-induced events that occur rapidly and/or at lower concentrations from those that occur only after longer and/or higher dose treatments. With respect to rapid regulation of DAT by palmitoylation, we found in synaptosomes that DAT displayed [³H]palmitate labeling within 90 min and that 2BP inhibited palmitoylation by ~40% within 45 min, demonstrating that palmitate turnover is rapid and capable of functioning as a mechanism for acute transporter regulation. Lower dose/shorter duration 2BP treatments led to strongly reduced DA transport V_{max} with little to no loss of DAT protein, and this effect occurred in the absence of endocytosis, indicating that in the short term, reduction of palmitoylation decreases transport kinetic efficiency. With respect to longer term regulation of DAT by palmitoylation, we found that higher dose/longer duration 2BP treatments in both synaptosomes and cells caused DAT protein losses and that these treatments and C580A mutation resulted in production of DAT degradation fragments, supporting an additional role for palmitoylation in opposing DAT turnover. It is noteworthy that in previous studies on DAT degradation, transporter losses were obtained only in the presence of cycloheximide plus PMA (13, 16, 18). Thus, the DAT losses and degradation fragments produced in this study in the absence of protein synthesis inhibitors or PKC activation strongly support palmitoylation as a major force opposing DAT turnover. We also found that down-regulation of transport induced by PMA and 2BP in both synaptosomes and cells was additive, indicating that PMA and 2BP effects on transport occur by independent mechanisms and that C580A DAT displayed increased PMA-stimulated down-regulation compared with WT DAT, indicating that palmitoylation of DAT opposes PMA-induced transport down-regulation. Thus, conditions that modify DAT palmitoylation could impact transporter responsiveness to regulatory signals by opposing or enhancing PKC-mediated effects. Together these findings indicate that palmitoylation of DAT functions to promote DA transport capacity in the short term through

increased transport kinetics and opposition to PKC-induced down-regulation and in the longer term through suppression of DAT degradation. Conditions that affect DAT palmitoylation could thus have a significant short and long term impact on DA neurotransmission and potentially be related to dopaminergic disorders.

Surprisingly, in these studies we found that induction of transport down-regulation by PMA was also retained in the absence of DAT endocytosis. PMA-induced internalization of DAT has been demonstrated many times in heterologous cell lines (12, 13, 16, 18, 21) and in synaptosomes (43), and it has generally been considered to represent the mechanism of DA transport down-regulation. In our study, the synaptosomes were maintained in high sucrose buffer during the 2BP and PMA pretreatments to extend their viability. As high sucrose blocks endocytosis, our findings demonstrate that down-regulation of DAT by PKC in synaptosomes is achieved independently of internalization. We previously identified a nonendocytotic component to PKC-induced DA transport down-regulation in LLCPK$_1$ cells associated with cholesterol-rich microdomains (21), and trafficking independent regulation of DAT by amphetamine has also been reported (44), further supporting kinetic mechanisms in regulation of transport.

A major difference we found for DAT palmitoylation characteristics in synaptosomes and heterologous cells was that V_{max} was acutely reduced by 2BP in synaptosomes, but it was not changed in the C580A mutant or in expressed DATs given 2BP treatment when activity was normalized for DAT levels. Further work will be necessary to identify the source of these differences, but we speculate that the retention of palmitoylation on the unidentified site of C580A DAT suffices to support some palmitoylation-dependent functions that are affected by 2BP in synaptosomes. It is also possible that LLCPK$_1$ cells and neurons possess different DAT palmitoylation enzymes with different 2BP sensitivities or possess different membrane lipid/protein environments that differentially impact palmitoylation-dependent functions. We also typically found in cells that 2BP induced greater losses of DAT protein relative to losses of transport activity. This could occur if internal DAT pools are lost to a greater extent than surface pools, although this remains to be tested. With respect to other characteristics of C580A DATs, we found that the protein undergoes full maturation and shows steady-state surface levels comparable with the WT form, demonstrating that palmitoylation of Cys-580 is not required for DAT biosynthesis or surface targeting. However, at present, we cannot exclude the possibility that palmitoylation remaining on C580A DAT suffices to support these or other functions, and full determination of palmitoylation effects on DAT biosynthesis, maturation, and other properties will require identification of the additional site(s).

Our results strongly support Cys-580 at the intracellular end of TM12 as a major palmitoylation site on rDAT. The analogous Cys residue is conserved in human and mouse DAT (45–47), indicating the potential for the site to be modified in all isoforms. Usage of this site is consistent with the commonly seen palmitoylation pattern for multiple pass

membrane proteins at the intracellular membrane boundary of the most C-terminal transmembrane domain (48). Molecular modeling of DAT suggests that TM12 consists of residues 556–585 that form a lengthy continuous α-helix that extends intracellularly past the lipid bilayer, with Cys-580 found several residues from the end of the helix near the membrane-cytoplasm interface (see Fig. 6A) (49). Thus, although palmitoylation of some proteins such as G-protein-coupled receptors and ion channels occurs many residues downstream of the membrane-cytoplasm interface and allows for stabilization of cytoplasmic loops (50), the presence of Cys-580 within a helix and close to the membrane-cytoplasm transition indicates that this may not be the case for DAT.

How Cys-580 palmitoylation impacts TM12 structure and DAT function are not known. Based on homology to the bacterial LeuT leucine transporter, DAT TM12 is predicted to be positioned outside the active transport core generated by TM1–10 and play no direct role in substrate permeation (49, 51). This is consistent with the lack of kinetic effects found for the C580A mutant, and it may indicate that the reduced transport V_{max} seen in 2BP-treated synaptosomes is mediated via the currently unknown palmitoylation site(s), whereas degradation effects are more clearly associated with Cys-580. Identification of the additional palmitoylation site(s) will be necessary to test these ideas, but differential functional effects mediated by distinct palmitoylation sites have been found for other proteins (52). Other possibilities for function of Cys-580 palmitoylation include impacts on DAT oligomerization (53), as TM12 of LeuT forms a dimer interface, and palmitoylation has been suggested to stabilize protein dimeric interactions (54, 55) or targeting of DAT to membrane rafts (20, 21).

With respect to regulation of DAT degradation by palmitoylation, the mechanism is also unclear. In cell systems, DAT undergoes degradation in lysosomes following PKC-induced internalization (13, 18), and several N- and C-terminal motifs of DAT have been linked to endocytotic trafficking and/or degradation. At the C terminus, these include a binding site for the scaffolding protein Hic5 at hDAT residues 571–580 adjacent to the potential hDAT palmitoylation site (56), C-terminal residues 587–596 that impact constitutive and PKC-dependent trafficking (8, 19, 57), and a distal C-terminal binding site for PICK1 that impacts transport surface targeting (58, 59). N-terminal mechanisms related to trafficking and degradation include ubiquitylation of N-terminal domain lysines necessary for PKC-induced endocytosis and degradation (18) and suppression of constitutive endocytosis by membrane-proximal residues (60). Whether the regulation of DAT entry into lysosomes by reduced palmitoylation is related to any of these mechanisms is not known.

S-Palmitoylation is becoming increasingly recognized as an important regulator of neuronal protein function (24), and the results presented in this study are the first to demonstrate palmitoylation of DAT or any other member of the SLC6 family of Na$^+$-Cl$^-$ dependent transporters for neurotransmitters and solutes. Many PAT and PPT enzymes are highly expressed in neurons and reversibly regulate the palmitoylation level of numerous proteins involved in neurotransmission and synaptic plasticity (24, 61–65). Twenty three mammalian

PATs have been identified (63), but little is currently known regarding mutations or regulatory abnormalities associated with disease states. Protein depalmitoylation is catalyzed by two PPT enzymes associated with lysosomes (66) and the cytoplasmic protein acyl-protein thioesterase (65). Many PPT mutations result in loss of substrate depalmitoylation necessary for lysosomal degradation (67, 68), leading to lysosomal storage diseases associated with neuronal dysfunction and death (69). Our results suggest that such mutations or dysregulation of DAT palmitoylation/depalmitoylation enzymes could profoundly affect short or long term function of DAT. As dopaminergic diseases such as Parkinson disease, schizophrenia, attention deficit hyperactive disorder, and drug abuse may result from inappropriate levels of DAT or DA clearance capacity, this suggests the potential for abnormal palmitoylation to be related to these disorders by impacting dopaminergic neurotransmission in both acute and chronic manners.

REFERENCES

1. Bannon, M. J., Sacchetti, P., and Granneman, J. G. (1998) in *Psychopharmacology. The Fourth Generation of Progress* (Bloom, K., ed) on-line edition, Raven Press, Ltd., New York
2. Giros, B., Jaber, M., Jones, S. R., Wightman, R. M., and Caron, M. G. (1996) *Nature* **379,** 606–612
3. Miller, G. W., Gainetdinov, R. R., Levey, A. I., and Caron, M. G. (1999) *Trends Pharmacol. Sci.* **20,** 424–429
4. Sotnikova, T. D., Beaulieu, J. M., Gainetdinov, R. R., and Caron, M. G. (2006) *CNS Neurol. Disord. Drug Targets* **5,** 45–56
5. Sulzer, D., Sonders, M. S., Poulsen, N. W., and Galli, A. (2005) *Prog. Neurobiol.* **75,** 406–433
6. Mortensen, O. V., and Amara, S. G. (2003) *Eur. J. Pharmacol.* **479,** 159–170
7. Zahniser, N. R., and Sorkin, A. (2009) *Semin. Cell Dev. Biol.* **20,** 411–417
8. Melikian, H. E. (2004) *Pharmacol. Ther.* **104,** 17–27
9. Loder, M. K., and Melikian, H. E. (2003) *J. Biol. Chem.* **278,** 22168–22174
10. Zahniser, N. R., and Sorkin, A. (2004) *Neuropharmacology* **47,** Suppl. 1, 80–91
11. Eriksen, J., Bjørn-Yoshimoto, W. E., Jørgensen, T. N., Newman, A. H., and Gether, U. (2010) *J. Biol. Chem.* **285,** 27289–27301
12. Melikian, H. E., and Buckley, K. M. (1999) *J. Neurosci.* **19,** 7699–7710
13. Miranda, M., Wu, C. C., Sorkina, T., Korstjens, D. R., and Sorkin, A. (2005) *J. Biol. Chem.* **280,** 35617–35624
14. Sorkina, T., Miranda, M., Dionne, K. R., Hoover, B. R., Zahniser, N. R., and Sorkin, A. (2006) *J. Neurosci.* **26,** 8195–8205
15. Kahlig, K. M., and Galli, A. (2003) *Eur. J. Pharmacol.* **479,** 153–158
16. Daniels, G. M., and Amara, S. G. (1999) *J. Biol. Chem.* **274,** 35794–35801
17. Sorkina, T., Richards, T. L., Rao, A., Zahniser, N. R., and Sorkin, A. (2009) *J. Neurosci.* **29,** 1361–1374
18. Miranda, M., Dionne, K. R., Sorkina, T., and Sorkin, A. (2007) *Mol. Biol. Cell* **18,** 313–323
19. Holton, K. L., Loder, M. K., and Melikian, H. E. (2005) *Nat. Neurosci.* **8,** 881–888
20. Adkins, E. M., Samuvel, D. J., Fog, J. U., Eriksen, J., Jayanthi, L. D., Vaegter, C. B., Ramamoorthy, S., and Gether, U. (2007) *Biochemistry* **46,** 10484–10497
21. Foster, J. D., Adkins, S. D., Lever, J. R., and Vaughan, R. A. (2008) *J. Neurochem.* **105,** 1683–1699
22. Resh, M. D. (2006) *Sci. STKE 2006,* re14
23. Huber, T. B., Schermer, B., Müller, R. U., Höhne, M., Bartram, M., Calixto, A., Hagmann, H., Reinhardt, C., Koos, F., Kunzelmann, K., Shirokova, E., Krautwurst, D., Harteneck, C., Simons, M., Pavenstädt, H., Kerjaschki, D., Thiele, C., Walz, G., Chalfie, M., and Benzing, T. (2006) *Proc. Natl. Acad. Sci. U.S.A.* **103,** 17079–17086
24. el-Husseini Ael-D., and Bredt, D. S. (2002) *Nat. Rev. Neurosci.* **3,** 791–802
25. Huang, K., and El-Husseini, A. (2005) *Curr. Opin. Neurobiol.* **15,** 527–535
26. Lever, J. R., Carroll, F. I., Patel, A., Abraham, P., Boja, J. W., Lewin, A. H., and Lew, R. (1993) *J. Labeled Compd. Radiopharm.* **33,** 1131–1137
27. Gu, H., Wall, S. C., and Rudnick, G. (1994) *J. Biol. Chem.* **269,** 7124–7130
28. Vaughan, R. A., Parnas, M. L., Gaffaney, J. D., Lowe, M. J., Wirtz, S., Pham, A., Reed, B., Dutta, S. M., Murray, K. K., and Justice, J. B. (2005) *J. Neurosci. Methods* **143,** 33–40
29. Jackson, C. S., and Magee, A. I. (1996) in *Current Protocols in Protein Science* (Chandra, V. B., and Leonard, S. A. eds) pp. 14.12.11–14.12.19, John Wiley & Sons, Inc., New York
30. Drisdel, R. C., Alexander, J. K., Sayeed, A., and Green, W. N. (2006) *Methods* **40,** 127–134
31. Kang, R., Wan, J., Arstikaitis, P., Takahashi, H., Huang, K., Bailey, A. O., Thompson, J. X., Roth, A. F., Drisdel, R. C., Mastro, R., Green, W. N., Yates, J. R., 3rd, Davis, N. G., and El-Husseini, A. (2008) *Nature* **456,** 904–909
32. Wan, J., Roth, A. F., Bailey, A. O., and Davis, N. G. (2007) *Nat. Protoc.* **2,** 1573–1584
33. Gaffaney, J. D., and Vaughan, R. A. (2004) *Mol. Pharmacol.* **65,** 692–701
34. Vaughan, R. A., and Kuhar, M. J. (1996) *J. Biol. Chem.* **271,** 21672–21680
35. Vaughan, R. A., Huff, R. A., Uhl, G. R., and Kuhar, M. J. (1997) *J. Biol. Chem.* **272,** 15541–15546
36. Dunkley, P. R., Jarvie, P. E., and Robinson, P. J. (2008) *Nat. Protoc.* **3,** 1718–1728
37. Parnas, M. L., Gaffaney, J. D., Zou, M. F., Lever, J. R., Newman, A. H., and Vaughan, R. A. (2008) *Mol. Pharmacol.* **73,** 1141–1150
38. Drisdel, R. C., and Green, W. N. (2004) *BioTechniques* **36,** 276–285
39. Jennings, B. C., Nadolski, M. J., Ling, Y., Baker, M. B., Harrison, M. L., Deschenes, R. J., and Linder, M. E. (2009) *J. Lipid Res.* **50,** 233–242
40. Kimmich, G. A., Randles, J., and Wilson, J. (1994) *Am. J. Physiol.* **267,** C1119–C1129
41. Plásek, J., and Sigler, K. (1996) *J. Photochem. Photobiol. B* **33,** 101–124
42. Blaustein, M. P., and Goldring, J. M. (1975) *J. Physiol.* **247,** 589–615
43. Chi, L., and Reith, M. E. (2003) *J. Pharmacol. Exp. Ther.* **307,** 729–736
44. Richards, T. L., and Zahniser, N. R. (2009) *J. Neurochem.* **108,** 1575–1584
45. Giros, B., el Mestikawy, S., Godinot, N., Zheng, K., Han, H., Yang-Feng, T., and Caron, M. G. (1992) *Mol. Pharmacol.* **42,** 383–390
46. Brüss, M., Wieland, A., and Bönisch, H. (1999) *J. Neural. Transm.* **106,** 657–662
47. Wu, X., and Gu, H. H. (1999) *Gene* **233,** 163–170
48. Nadolski, M. J., and Linder, M. E. (2007) *FEBS J.* **274,** 5202–5210
49. Beuming, T., Shi, L., Javitch, J. A., and Weinstein, H. (2006) *Mol. Pharmacol.* **70,** 1630–1642
50. Chini, B., and Parenti, M. (2009) *J. Mol. Endocrinol.* **42,** 371–379
51. Yamashita, A., Singh, S. K., Kawate, T., Jin, Y., and Gouaux, E. (2005) *Nature* **437,** 215–223
52. Hayashi, T., Thomas, G. M., and Huganir, R. L. (2009) *Neuron* **64,** 213–226
53. Hastrup, H., Karlin, A., and Javitch, J. A. (2001) *Proc. Natl. Acad. Sci. U.S.A.* **98,** 10055–10060
54. Woehler, A., Wlodarczyk, J., and Ponimaskin, E. G. (2009) *Glycoconj. J.* **26,** 749–756
55. Kobe, F., Renner, U., Woehler, A., Wlodarczyk, J., Papusheva, E., Bao, G., Zeug, A., Richter, D. W., Neher, E., and Ponimaskin, E. (2008) *Biochim.*

Biophys. Acta **1783,** 1503–1516

56. Carneiro, A. M., Ingram, S. L., Beaulieu, J. M., Sweeney, A., Amara, S. G., Thomas, S. M., Caron, M. G., and Torres, G. E. (2002) *J. Neurosci.* **22,** 7045–7054

57. Boudanova, E., Navaroli, D. M., Stevens, Z., and Melikian, H. E. (2008) *Mol. Cell. Neurosci.* **39,** 211–217

58. Torres, G. E., Yao, W. D., Mohn, A. R., Quan, H., Kim, K. M., Levey, A. I., Staudinger, J., and Caron, M. G. (2001) *Neuron* **30,** 121–134

59. Bjerggaard, C., Fog, J. U., Hastrup, H., Madsen, K., Loland, C. J., Javitch, J. A., and Gether, U. (2004) *J. Neurosci.* **24,** 7024–7036

60. Guptaroy, B., Zhang, M., Bowton, E., Binda, F., Shi, L., Weinstein, H., Galli, A., Javitch, J. A., Neubig, R. R., and Gnegy, M. E. (2009) *Mol. Pharmacol.* **75,** 514–524

61. Fang, C., Deng, L., Keller, C. A., Fukata, M., Fukata, Y., Chen, G., and Lüscher, B. (2006) *J. Neurosci.* **26,** 12758–12768

62. Keller, C. A., Yuan, X., Panzanelli, P., Martin, M. L., Alldred, M., Sassoè-Pognetto, M., and Lüscher, B. (2004) *J. Neurosci.* **24,** 5881–5891

63. Fukata, M., Fukata, Y., Adesnik, H., Nicoll, R. A., and Bredt, D. S. (2004) *Neuron* **44,** 987–996

64. Hayashi, T., Rumbaugh, G., and Huganir, R. L. (2005) *Neuron* **47,** 709–723

65. Duncan, J. A., and Gilman, A. G. (1998) *J. Biol. Chem.* **273,** 15830–15837

66. Lu, J. Y., and Hofmann, S. L. (2006) *J. Lipid Res.* **47,** 1352–1357

67. Vesa, J., Hellsten, E., Verkruyse, L. A., Camp, L. A., Rapola, J., Santavuori, P., Hofmann, S. L., and Peltonen, L. (1995) *Nature* **376,** 584–587

68. Linder, M. E., and Deschenes, R. J. (2003) *Biochemistry* **42,** 4311–4320

69. Gupta, P., Soyombo, A. A., Atashband, A., Wisniewski, K. E., Shelton, J. M., Richardson, J. A., Hammer, R. E., and Hofmann, S. L. (2001) *Proc. Natl. Acad. Sci. U.S.A.* **98,** 13566–13571